Moroccan Journal of Chemistry
ISSN: 2351-812X
http://revues.imist.ma/?journal=morjchem&page=login
Rahmat & al. / Mor. J. Chem. 10 N°4 (2022) 738-751
DOI: https://doi.org/10.48317/IMIST.PRSM/morjchem-v10i4.32146

Sawdust Essential Oil of *Cedrus Atlantica* as Eco-Friendly inhibitor against mild steel corrosion in 1M HCl solution

C. Bouyahia[(a)], M. SLAOUI[(b)]*, H. AL-Sharabi [(c,d)], H. El Bakraoui[(b)], S. El Hajjaji[(a)]

[(a)]Laboratory of Spectroscopy, Molecular Modeling, Materials, Nanomaterials, Water and Environment, CERNE2D, Faculty of Sciences, Mohammed V University in Rabat, Av Ibn Battouta, BP1014, Agdal, Morocco.
[(b)] Energy, materials and sustainable development (EMDD) Laboratory- Higher School of Technology - SALE. CERN2D Center. Mohammed V University in RABAT- Avenue des Nations Unies, B. P: 8007. N. U Agdal, Rabat.Morocco*
[(c)] Laboratory of Spectroscopy, Molecular Modeling, Materials, Nanomaterials, Water and Environment, CERNE2D, ENSAM, Mohammed V University in Rabat, Morocco
[(d)] Laboratory of chemistry, Jamal Abdulnasser High School, Ministry of Education,Yemen;

** Corresponding author: smslaoui@yahoo.fr*
Received 27 April 2022, Revised 03 sept 2022, Accepted 05 sept 2022

Abstract

The inhibition efficiency of wood sawdust essential oil of *Cedrus Atlantica* against mild steel corrosion in 1M HCl solution has been tested using electrochemical impedance spectroscopy (EIS) and Potentiodynamic polarization. Polarization measurements revealed cathodic-type inhibitor behavior. The inhibitory efficacy assessed by both polarization and (EIS) techniques was in typical agreement, with %IE values of 95.09 5% and 95.82 % at 250 ppm of oil essential. Based on the kinetic and thermodynamic properties K_{ads} and $\triangle G°_{ads}$, it is concluded that WSCA oil adsorption occurs via a physisorption process and follows the Langmuir isotherm. In addition, the temperature effect was studied at (303–333 K), and the thermodynamic parameters (E_a, $\triangle H$, $\triangle S$) were determined and discussed to elaborate the corrosion mechanism. The corrosion inhibition effect was discovered to be temperature and inhibitor concentration dependent.

Keywords:*Mild steel, wood sawdust, Essential oil, Cedrus Atlantica, EIS, Tafel, Corrosion,1M HCl.*

1. Introduction

Corrosion is a point of interest to interdisciplinary research groups because it combines materials science, chemistry, physics, metallurgy, and chemical engineering [1-3]. Corrosion is caused by the action of an environment on metals and alloys, both chemically and electrochemically. The consequences are significant in a variety of fields, particularly industry: production halts, replacement of corroded parts, accidents, and pollution risks are all common occurrences with sometimes-severe economic consequences [4,5]. As a result, the development of steel inhibitors in acid solutions has piqued the interest of many researchers, particularly in terms of efficiency and applications [6, 7]. Because of the varying corrosive environments in these systems, the selection and application of inhibitors is actually complicated. The majority of the *Cedrus Atlantica* is one of the most economically and ecologically important species in Morocco's Mediterranean mountains [8]. This species grows primarily in cold sub-humid, humid, and per-humid climatic environments; its bioclimatic optimum corresponds to the Mediterranean mountainous stage between 1600 and 2000 m. It is a conifer tree of the Pinaceae family that can grow to a height of 30 to 40 m [9]. The purpose of this study is to test wood sawdust essential oil from *Cedrus Atlantica* as a corrosion inhibitor for mild steel in a 1 M HCl solution. Electrochemical polarization methods are used in the research. To investigate the mechanism of corrosion inhibition, polarization curves and electrochemical impedance spectroscopy were used.

2. Materials and methods

2.1. Plant extracts preparation

The sawdust samples were collected from a sawmill in Azrou (Middle Atlas). The grinding process was used until a fine powder was obtained. Extraction by hydro distillation: A flask is filled with water and 100 g of sawdust. It is installed in the Clevenger apparatus for 6 hours. The mixture (oil and water) is separated by density difference. The recovered oil is stored in a small opaque bottle in the refrigerator.

2.2. GC-MS analysis

Gas chromatography with mass spectroscopy was used to identify the constituents. The device is a Perkin Elmer Version ClarusTM GC-680 with Q-8 MS. It includes an auto-sampler for automatic sample injection into the injector, as well as a RxiR-5Sil MS type capillary column traversed by Helium gas. The mass spectrometer is powered by a SMART source of electronic ionization, which allows it to ionize and vaporize various molecules, as well as a quadrupole filter that separates the various ions based on their m/z ratio. The GC-MS system is run by a computer with Turbomass TM software, which allows for the programming of analysis methods as well as the qualitative and quantitative identification of the species detected. With a gas flow rate of 1 mL/min, the analysis takes 2 hours. The energy of ionization was 70 eV. At 260° C, a volume of 0.5 L was injected. The oven temperature program begins at 40 degrees Celsius for 2 minutes, and then rises at a rate of 10 degrees Celsius per minute to 290 degrees Celsius.

2.3. Electrode and solution corrosive

Mild steel, which was used in this study, has the following composition: 0.09 wt% P, 0.38 wt% Si, 0.01 wt% Al, 0.05 wt% Mn, 0.21 wt% C, 0.05 wt% S, and the remainder iron. Electrochemical measurements were performed on the specimen. 1cm^2 of exposed surface area Surface preparation was performed with emery papers of increasing grades (400, 600, and 1200 grit size), followed by degreasing with AR grade ethanol and drying at room temperature before use. The 1M HCl aggressive solutions were made by diluting analytical grade 37 % HCl with double distilled water.

2.4. Electrochemical measurements

The electrochemical assays were made out in a stationary position using a Volta lab (Tacussel- Radiometer PGZ 100) potentiostat and Tacussel corrosion analysis software model (Voltamaster 4). A three-electrode corrosion cell was used. A saturated calomel electrode served as the reference electrode for this experiment (SCE). As an auxiliary electrode, a one-centimeter-square platinum electrode was used. Carbon steel with a surface area of 1 cm2 served as the working electrode. This reference electrode was used as the basis for all potentials in this study. A steady state open circuit potential was established by immersing the working electrode in test solution for 30 minutes (Eocp). The electrochemical process was carried out after the Eocp measurements. In aerated solutions, all electrochemical tests were carried out. The potential applied to the sample was continuously varied at Potentiodynamic polarization measurements on a mild steel substrate in inhibited and uninhibited solution were scanned from cathodic to anodic direction at a rate of 2 mV/s. The polarization Volta Master 4 software was used to analyze the Potentiodynamic data. To obtain corrosion current densities (i_{corr}), the linear Tafel segments of anodic and cathodic curves were extrapolated to corrosion potential (E_{corr}). The inhibition efficiency (%IE) was calculated using the following relationship from the measured Icorr values [10], (1):

$$\%IE_{PDP} = (i^{\circ}_{corr} - i^{inh}_{corr}/i^{\circ}_{corr}) \times 100 \qquad (1)$$

Where i°_{corr} and i^{inh}_{corr} are the steel corrosion current density values obtained by extrapolating Tafel lines without and with the inhibitor added, respectively.

The EIS experiments were carried out in the frequency range with a high limit of 100 kHz and different low limits of 0.1 Hz at open circuit potential, with 10 points per decade, at the rest potential, after 30 minutes of acid immersion, by applying a 10 mV ac voltage peak-to-peak. These experiments resulted in the creation of Nyquist plots. The best semicircle can be fit through the data points in the Nyquist plot using a non-linear least square fit to give the intersections with the x-axis. Using the following equation, the inhibitor's inhibition efficiency was calculated based on the charge transfer resistance values [3,11]:

$$\%IE_Z = (R^{inh}_{ct} - R^{\circ}_{ct}/R^{inh}_{ct}) \times 100 \qquad (2)$$

Where R^{inh}_{ct} and R°_{ct} are respectively the values of the charge transfer resistances of the mild steel in 1M HCl with and without the different concentrations of WSCA oil.

3. Results and discussion

3.1. Chemical composition of WSCA oil

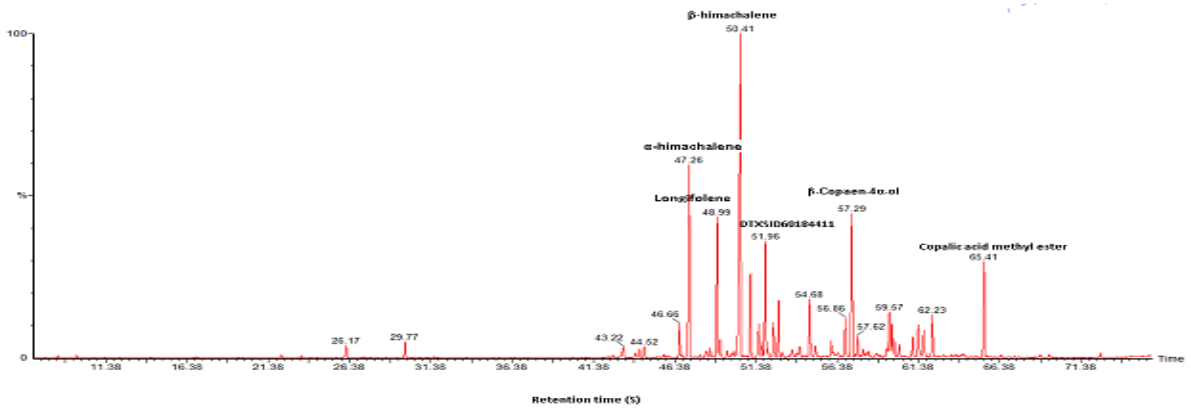

Figure 1. *GC-MS chromatogram of WSCA oil*

Table 1. Chemical composition of WSCA oil

Compound	TR	%
P-Cresol	22.189	0.12
Endo-borneol	28.597	0.02
(+)-Calarene	44.211	0.37
Farnesol	46.656	1.43
α-himachalene	47.263	**9.4**
Longipinene	_	_
Longifolene	48.99	**6.74**
β-himachalene	50.415	**21.32**
1-Mesitylbuta-1.3-diene	51.032	**3.77**
δ-Cadinene	_	_
E-Calamenene	51.542	1.73
α-Calacorene	51.756	0.62
DTXSID60184411	51.956	**5.31**
DTXSID80344212	54.678	3.09
Androstenediol	55.021	0.66
Longiborneol	56.005	0.91
(-)-Isolongifolol	56.862	2
β-Copaen-4α-ol	57.28	**7.71**
α-Cubebene	57.62	0.9
(+)-gamma-Gurjunene	58.283	0.24
Acoradiene	58.787	0.28
β-humulene	59.571	1.83
Carveol	59.731	1.01
Ledane	59.874	0.65
Cadalene	60.201	0.66
Cedreanol	61.25	3.32
Curlone	61.375	**3.69**
Tumerone	62.05	0.03
Tujopsene	62.223	1.95
Longipinane	62.77	0.04
β-cis-caryophyllene	63.4	0.11
Copaen-15-ol	64.86	0.07
Copalic acid methyl ester	65.408	**4.54**
Trans-Calamenene	65.59	0.07
Octasiloxane	_	_
Total		**84.57%**

Figure 1 and Table 1 show the chemical composition of the WSCA oil. These analyses led to the identification of approximately 32 components, which account for approximately 84.57% of the total WSCA oil composition. The main compound being: β-himachalene (21.32%) followed by α-himachalene (9.40%). The chemical analysis obtained has constituents relatively similar to those of other cedar wood analyzed by Aberchane and al. They discovered that the major compounds are β-himachalene (39.72%), α-himachalene (15.78%) γ-himachalene (9.56%) and E-α-atlantone (9.15%) Furthermore, the study conducted by Jaoudi and colleagues on WSCA oil of *C. atlantica* (in the provinces of Morocco's Middle Atlas in the forest of Itzer) found that the main compounds identified were: α-himachalene (24.25%), β-himachalene (13.76%), methyl-1,4-cyclohexadiene (9.06%), trans-cadina-1(6),4-diene (7.65%), and 6-camphenol (7.44%) [12-13].

3.2. Electrochemistry tests

3.2.1. Concentration effect

a. Polarization test

Figure 2 depicts Potentiodynamic anodic and cathodic polarization plots for mild steel specimens in 1 M HCl solution in the absence and presence of various concentrations of WSCA oil at ambient temperature. Table 2 shows the kinetic parameters such as corrosion current density (i_{corr}), corrosion potential (E_{corr}), cathodic and anodic Tafel slopes (c, a), and inhibition efficiency (IE %)

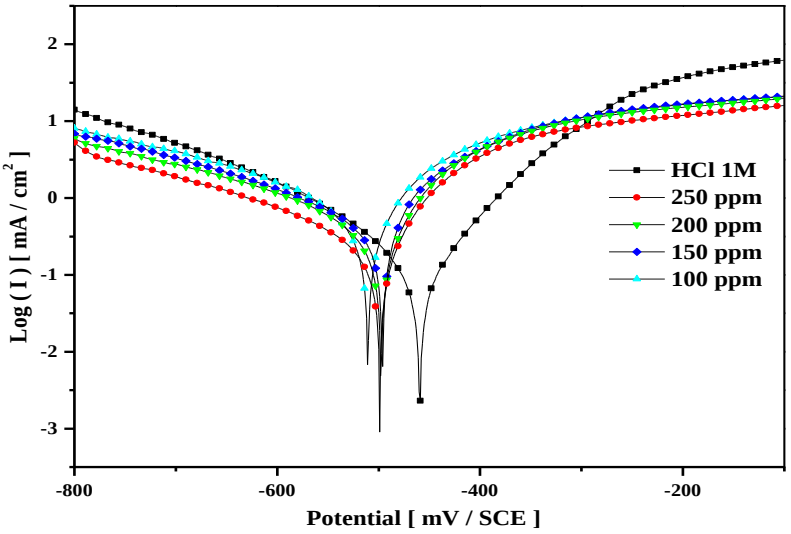

Figure 2. Anodic and cathodic polarization curves of mild steel in 1M HCl medium with and without the addition of different concentration of WSCA oil.

In the cathodic domain (Fig. 2), it is clear that the cathodic current density decreases with the addition of WSCA oil; this could imply that the WSCA oil is adsorbed on the metal surface, causing inhibition. In the anodic domain (Fig. 2), the inhibition mechanism of WSCA oil was discovered to be electrode potential dependent. The presence of WSCA oil appears to have no effect on the anodic current den. Only after -300 mV/s does the inhibitor begin adsorption on the surface and the effect appears. These findings suggested that WSCA oil-primarily functions as a mixed inhibitor, with predominance in the cathodic part [14-16]. The corrosion parameters such as corrosion potential (E_{corr}), corrosion current density (i_{corr}), and the anodic cathodic Tafel slopes and inhibition efficiency were determined from the

polarization plots (Fig2) and are shown in table 2 where the cathodic (βc) and anodic (βa) slopes improved slightly when the inhibitor was added, indicating that the effect of WSCA on the kinetics of hydrogen evolution as well as its adsorption on the mild steel.

Table 2. Polarization parameters for the mild steel in 1M HCl solutions with various concentration of WSCA oil.

Concentration	E_{corr} (mV/SCE)	i_{corr} (mA/cm^2)	β_c (mV)	β_a (mV)	IE_{PDP} (%)
1M HCl	-458.596	0.612	255.4	140.4	-
100 ppm	-509.708	0.131	160.8	90.0	78.59
150 ppm	-495.174	0.047	83.1	43.4	92.32
200 ppm	-495.545	0.036	83.7	39.9	94.11
250 ppm	-496.948	0.030	103.7	45.7	95.09

According to Table 2, the WSCA oil significantly improves the inhibition efficiency for mild steel depending on the corrosion current comparison without and with the oil under study [17,18].

b. Electrochemical Impedance Spectroscopy (EIS)

Fig. 3 depicts the Nyquist plots generated by the EIS investigation on mild steel in a 1M HCl medium with and without different varying WSCA oil concentrations. As shown in Figure 3, the impedance spectra of uninhibited and inhibited 1 M HCl solutions exhibit a single capacitive loop, indicating that steel corrosion is primarily controlled by the charge transfer process. These capacitive loops are not perfect semicircles, which can be attributed to the frequency dispersion effect caused by the roughness and inhomogeneity of the electrode surface. Furthermore, in the presence of an inhibitor, the diameter of the capacitive loop is larger than in blank solution and increases with inhibitor concentration [9,19,20].

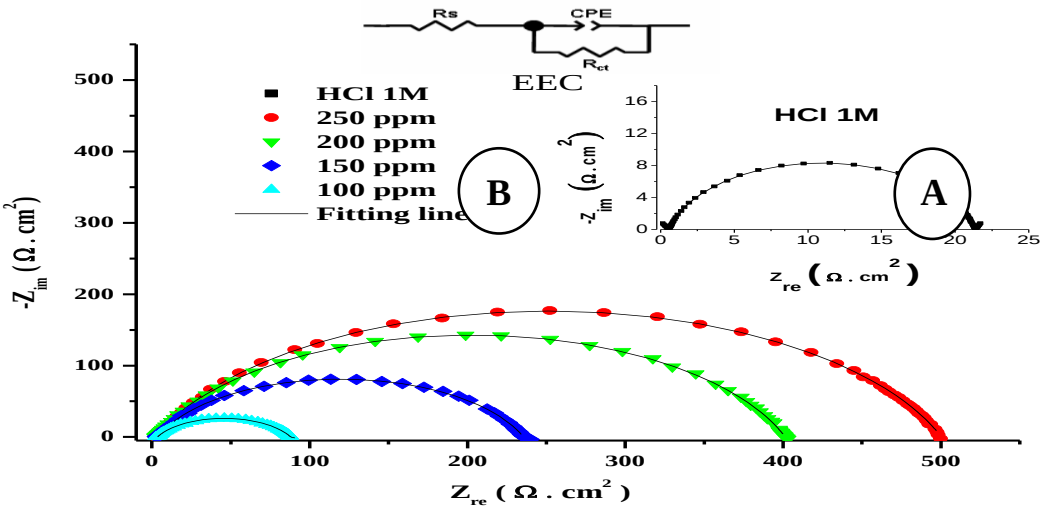

Figure 3. Nyquist plots of mild steel in 1M HCl **(A)** and 1M HCl with different concentrations of WSCA oil **(B)**.

An equivalent electrical circuit (EEC) illustrated in Fig3 was utilized to obtain data of electrical chemistry parameters of curves Nyquist. The utilized EEC was found to have an excellent correlation between experimental and simulated

graphs, with a coefficient of approximately 10^{-3} to 10^{-2}. In the analogous circuit (fig3), R1, R2, Q represent the electrolyte resistance, charge transfer resistance, and constant phase element reflecting the capacity of the double layer at the metal/solution interface in EEC. Instead of a double layer capacity (Cdl), "Q" was used to account for non-ideal behavior on the mild steel surface caused by inhomogeneity, roughness, porosity, and adsorption [9, 19, 20].

Table 3. ***Electrical parameters obtained by fitting the Nyquist curves of mild steel in 1M HCl without and with S WSCA oil.***

Concentration	R_s (Ω.cm2)	R_{ct} (Ω.cm2)	Q (F/cm^2). 10^{-6}	n	χ^2	IE_Z (%)
1M HCl	3.561	20.81	0.0047848	0.85998	0.0078	-
100 ppm	3.406	84.46	0.0024302	0.7043	0.0081	75.36
150 ppm	3.243	232.2	0.0010819	0.77622	0.0066	91.03
200 ppm	2.417	398.9	0.0008315	0.79091	0.0052	94.78
250 ppm	2.577	497.9	0.0007806	0.78475	0.0049	95.82

Indeed, according to the Helmholtz model's concept of double layer capacity, the more the inhibitor adsorbs, the thicker the organic deposition gets and the lower the double layer capacity becomes, as shown in equation (3)[21], [22]:

$$C_{dl} = \frac{\varepsilon \varepsilon_0}{e} S \qquad (3)$$

Where (e) is the thickness of the protective layer, (S) is the electrode surface area, Ɛ◦ is the medium permittivity, and (Ɛ) is the dielectric constant. Table 3 shows the values obtained from processing the Nyquist curves with the electrical circuit depicted in Figure 3. According to table 3, the addition of the WSCA oil appears to have a minor effect on the electrolyte resistance (Rs), indicating that the inhibitor used meets the requirement of being reliable without changing the physicochemical parameters of the solution. While the addition of the WSCA oil causes an increase in charge transfer resistance, demonstrating the inhibitor's protective effect against mild steel corrosion. Additionally, a decrease in values of Q, which is associated with the formation of a double-layer capacitor, indicates a decrease in the dielectric constant, and thus an increase in the thickness of the double layer, in accordance with Helmholtz's model (eq.3) [3]. Moreover, we discover that as the concentration increases, so does the efficiency of inhibition, IE (%) increase. This confirms the Potentiodynamic polarization results [4, 23].

3.2.2 Adsorption isotherms

The electronic properties of the inhibitor, the nature of the metal surface, temperature, steric effects, and the varying degrees of surface-site activity all influence the adsorption process [24]. Indeed, the steel interface, H2O molecules from the solvent could be adsorbed. Adsorption of inhibitor molecules from aqueous solutions can thus be viewed as a quasi-substitution process between the oil (sol) in the aqueous phase and water molecules at the electrode surface [7;25;26]:

$$Oil_{(sol)} + b\ H_2O_{(ads)} \rightleftharpoons Oil_{(aq)} + b\ H_2O_{(sol)} \qquad (I)$$

Where b is the size ratio, that is, the number of water molecules re-placed by oil of WSCA.

The interaction force between the metal and the inhibitor must be greater than the interaction force between the metal and the water molecule to achieve effective inhibitor adsorption on a metal surface. To comprehend corrosion

adsorption processes, adsorption isotherms can be used. In this study, the Langmuir isotherm was used to explain the adsorption of WSCA essential oil on a mild steel surface [24]: $C/\theta = 1/k_{ads} + c$ (Eq 4)

Where θ is the surface coverage, K is the adsorption–desorption equilibrium constant, C is the concentration of inhibitor.

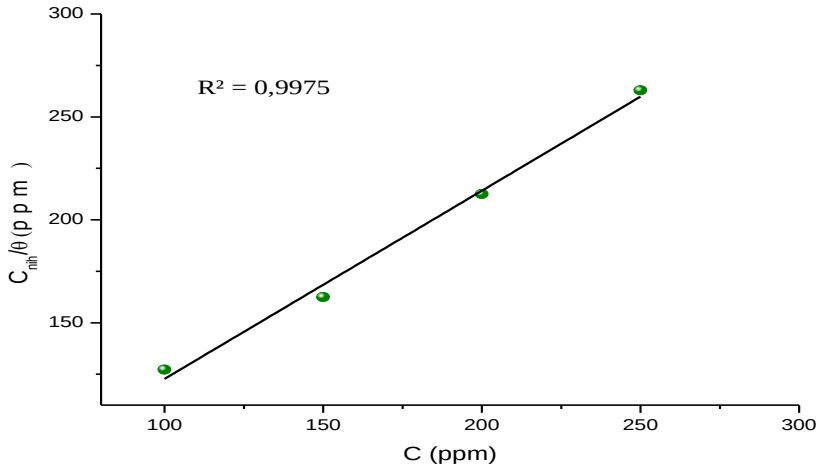

Figure 4. Langmuir adsorption isotherm of mild steel in HCl 1M in the presence of different concentrations of WSCA oil.

Figure 4 clearly shows that oil adsorption on the surface is subject to Langmuir adsorption, with R^2=0.9975. The Langmuir model assumes that an adsorbate inhibitor monolayer is positioned on a homogeneous solid surface, that there are no interactions between the adsorbate molecules, that an adsorbate molecule is fixed, that all surface sites are equivalent, and that each inhibitor molecule occupies a single active site without distinguishing between anode and cathode sites [7]. To determine the adsorption type, the free energy value is commonly used. The equation (10) describes the standard adsorption free energy (ΔG°ads) and the adsorption process equilibrium constant (Kads) [27-29]:

$$\Delta G°_{ads} = -2.303\ RT \log(55.5 K_{ads}) \quad (5)$$

Where R is the universal gas constant, T is the absolute temperature and 55.5 is the molar concentration of water (mol/L). The calculated value of $\Delta G°_{ads}$ was equal to -9.7 KJ/mol. This negative value indicates that WSCA is adsorbing spontaneously on the mild steel surface. The absolute value of $\Delta G°_{ads}$ is less than 20 kJ.mol^{-1}, meaning that the inhibitor's adsorption process on the mild steel surface involves electrostatic interactions [25;30;31].

3.2.3 Temperature Effect

The rate of corrosion of mild steel was investigated at temperatures ranging from 303 K to 333 K in the presence and absence of 250 ppm of WSCA oil. Temperature is one of the variables that can affect a material's behavior in a corrosive environment, as well as the metal-inhibitor interaction. Polarization measurements are investigated at various temperatures for this purpose, as well as the associated corrosion parameters and inhibition efficiency, as well as thermodynamic parameters [27;32]. Table 4 and Figure 5 show the final results. Table 4 shows that the corrosion rate of steel increases with temperature both in the absence and presence of inhibitor at a concentration of 250 ppm, but the effect is more noticeable in the blank solution, and the inhibition efficiency values decrease with increasing temperature. This decrease in inhibition efficiency when the solution temperature is raised could be attributed to an increase in the mobility of the inhibitor molecules, which reduces the interaction between the metallic surface and the

inhibitor molecules [33,34]. Following Equation 6, the Arrhenius equation can be successfully used to explain the effect of temperature on the inhibition performance of studied oil essential [32-35].

$$i_{corr} = A \exp\left[{}^{-E_a}/_{RT}\right] \quad (6)$$

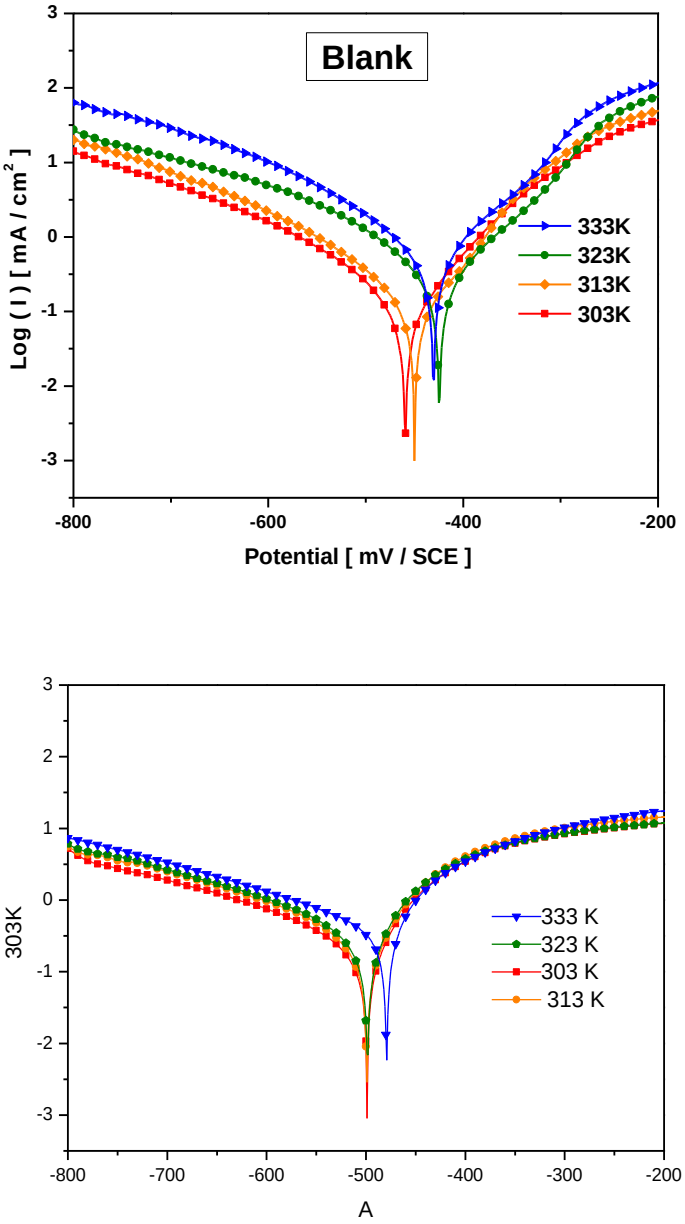

Figure 5. Tafel plots for mild steel in 1M HCl (Blank) and with 250 ppm (Inhibitor) of WSCA oil at 303-333K.

Where A is Arrhenius constant, E_a denotes the apparent activation energy, R is the ideal gas constant, and T represents the absolute temperature. Table 4 shows the values of apparent activation energy of corrosion E_a and pre-exponential factor (A) for mild steel in 1 M HCl with and without inhibitor, calculated using linear regression by plotting the values of ln (i_{corr}) versus (1/T).The following is an alternative formulation of the Arrhenius equation (Eq 7) [36]:

$$i_{corr} = \frac{RT}{Nh} \exp{}^{\Delta S_a}/_{R} \; exp^{\,-\Delta H_a}/_{RT} \quad (7)$$

Where N signifies the Avogadro number, h denotes Planck's constant, R symbolizes the universal gas constant, ΔHa represents the activation enthalpy, and ΔSa exemplifies the activation entropy.For all of the inhibitor concentrations studied the plots of ln (i_{corr}) vs. 1/T and ln (i_{corr}/T) vs. 1/T yielded straight lines with linear regression coefficients close to unity

Table 4. ***The parameters electrochemical of the temperature effect for mild steel corrosion in 1 M HCl and with 250 ppm of WSCA at 303-333K.***

Medium	Temperature (K)	E_{corr} (mV/SCE)	βc (mV/s)	βa (mV/s)	I_{corr} (mA/cm^2)	IE (%)
Blank	303	-458.59	255.4	140.4	612.37	-
	313	-450.99	255.1	128.8	867.56	-
	323	-429.33	367.08	158.2	1439.25	-
	333	-428.24	384.6	184.0	2042.07	-
WSCA	303	-496.95	103.7	45.7	30.02	95.09
	313	-497.59	219.2	102.4	96.21	88.91
	323	-497.96	268.9	109.6	143.69	90.00
	333	-478.05	356.7	141.2	279.79	86.29

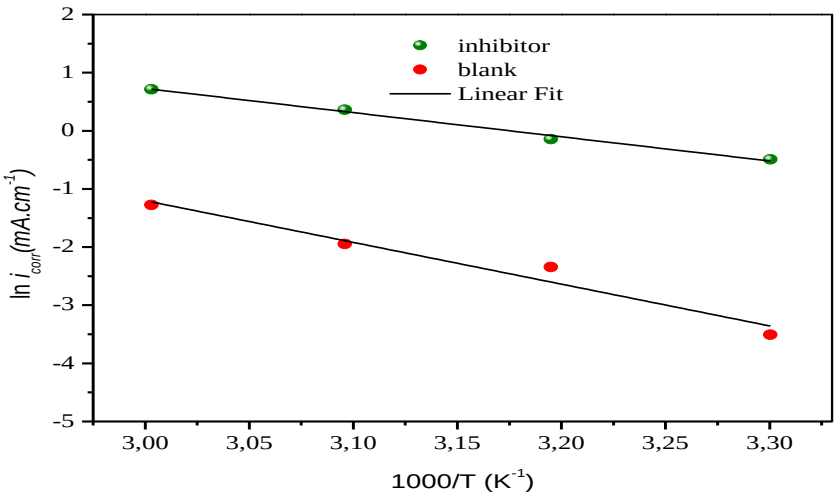

Figure 5. Arrhenius plots of ln Icorr in 1 M HCl in the absence and presence of WSCA at 250 ppm.

The data in Table 5 showed positive trends for both Ea and ΔHa, suggesting that the corrosion process is endothermic. The activation energy and enthalpy of activation are clearly increased in the presence of the inhibitor, implying that the corrosion reaction's energy barrier is raised. The negative sign for activation entropy in both inhibited and uninhibited solutions indicates that the activation complex in the rate-determining step denotes association rather than dissociation, implying a decrease in disorder ness from reactant to activated complex. This mechanism could be explained as follows: the adsorption of WSCA molecules from the aqueous solution can be thought of as a quasi-

substitution process between the organic compound in the aqueous phase and water molecules at the electrode surface. As in the chemical equation (I) aforementioned. Where the adsorption of WSCA is accompanied by the desorption of water molecules from the surface in this situation [33, 36].

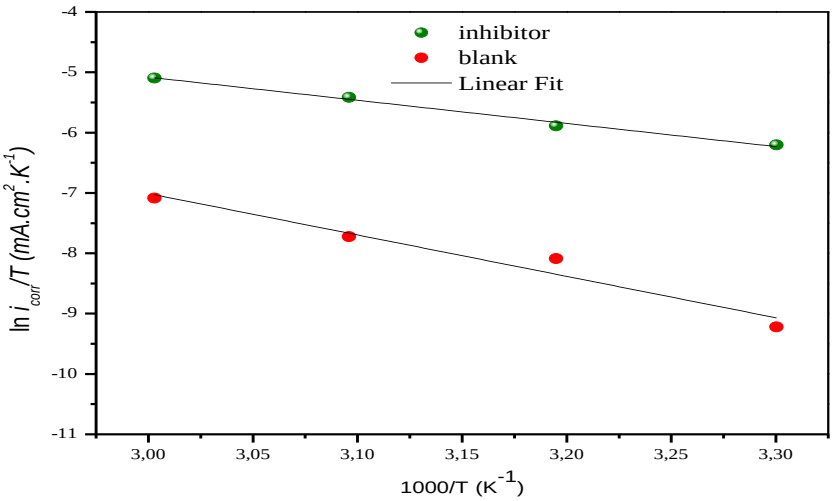

Figure 6. Transition-state plots for mild steel corrosion current (Icorr) in 1 M HCl with and without 250 ppm WSCA oil.

Table 5. ***Thermodynamique parameters***

Solutions	**Ea**	**ΔHa**	**-ΔSa**
	(kJ·mol^{-1})	**(kJ·mol^{-1})**	**(kJ·mol^{-1} k^{-1})**
Blank	34.55140	31.91220818	144.0410
WSCA	59.69476	57.05557326	84.65397

Conclusion

The corrosion behavior of mild steel in a 1M HCl medium was evaluated using various concentrations of a green inhibitor. The adsorption of these inhibitor molecules on the steel surface, according to the findings, slows the corrosion process. The polarization measurements revealed that the added oil acted as a cathodic-type inhibitor, with inhibition efficiencies (IE) determined by both polarization and EIS methods being in good agreement, and an IE value of 95 % was obtained with 250 ppm of the WSCA. The Langmuir adsorption isotherm was successfully used to describe the adsorption of WSCA, and the corresponding value of $\Delta G°_{ads}$ revealed that the adsorption mechanism of this inhibitor on mild steel surfaces in 1 M HCl is primarily due to physisorption. Because of the higher dissolution of mild steel at higher temperatures, the inhibition efficiency decreased with increasing temperature, and the addition of WSCA increases the activation energy of the corrosion process.

References

[1] Bouhlal, F., Labjar, N., Abdoun, F., Mazkour, A., Serghini-Idrissi, M., El Mahi, M., Lotfi., El Hajjaji, S. "Electrochemical and thermodynamic investigation on corrosion inhibition of C38 steel in 1M hydrochloric acid using the hydro-alcoholic extract of used coffee grounds". International Journal of Corrosion, (2020) 1-4.

[2] A. Batah, M. Belkhaouda, L. Bammou, A. Anejjar, R. Salghi, A. chetouani, L. Bazzi, B. Hammouti, Corrosion

inhibition of carbon steel in acidic medium by Grapefruit oil extract, Mor. J. Chem. 5 N°4 (2017) 580-589

[3] Y. El aoufir, Y. El Bakri, Y. Kerroum, H. Lgaz, A. Harmaoui, A. Chetouani, J. Sebhaoui, R. Salghi, Y. Ramli, A. Guenbour, E.M. Essass, H. Oudda, Triazole derivative as new and effective corrosion inhibitor for carbon steel in hydrochloric acid: Electrochemical and quantum chemical studies, Mor. J. Chem. 5 N°4 (2017) 545-559

[4] K. Bouyad, Y. Kandri Rodi, H. Elmsellem, E. H. El Ghadraoui, Y. Ouzidan, I. Abdel-Rahman, H.S. Kusuma, I. Warad, J.T. Mague, E.M. Essassi, B. Hammouti, A. Chetouani, Imidazo[4,5-b]pyridines as a New Class of Corrosion Inhibitors for Mild Steel: Experimental and DFT Approach, Mor. J. Chem. 6N°1 (2018) 22-34

[5] Damej, M., Kaya, S., Ibrahimi, B. E., Lee, H. S., Molhi, A., Serdaroğlu, Lgaz, H., "The corrosion inhibition and adsorption behavior of mercaptobenzimidazole and bis-mercaptobenzimidazole on carbon steel in 1.0 M HCl: Experimental and computational insights", Surfaces and Interfaces, 24, (2021), 101095.

[6] Aiboudi, M., Yousfi, F., Fekkar, G., Bouyazza, L., Ramdani, M., El Azzouzi, M., Abdel-Rahman, I. "Eco-friendly Allium cepa L. seeds extracts as corrosion inhibitor for mild steel in 1 M HCl solutions". J. Mater. Environ. Sci, 10(4), (2019), 339-346.

[7] M. Kissi, M. Bouklah, B. Hammouti, and M. Benkaddour, "Establishment of equivalent circuits from electrochemical impedance spectroscopy study of corrosion inhibition of steel by pyrazine in sulphuric acidic solution", *Applied Surface Science*, 252 (12), (2006), 4190–4197.

[8] A. Terrab, O. Paun, S. Talavera, K. Tremetsberger, M. Arista, and T. F. Stuessy, "Genetic diversity and population structure in natural populations of Moroccan Atlas cedar (Cedrus atlantica; Pinaceae) determined with cpSSR markers", *American Journal of Botany*, 93 (9), (2006), 1274–1280.

[9] M.Coudel, P.M. Aubert, M. Aderghal, and C. Hély, "Pastoral and woodcutting activities drive Cedrus atlantica Mediterranean forest structure in the Moroccan Middle Atlas", Ecological Applications, 26 (2), (2016), 574–586.

[10] Belarbi, N., Dergal, F., Chikhi, I., Merah, S., Lerari, D., Bachari, K. "Study of anti-corrosion activity of Algerian L. stoechas oil on C38 carbon steel in 1 M HCl medium". International Journal of Industrial Chemistry, 9(2), (2018). 115-125.

[11] Bouklah, M., Benchat, N., Aouniti, A., Hammouti, B., Benkaddour, M., Lagrenée, Bentiss, F. "Effect of the substitution of an oxygen atom by sulphur in a pyridazinic molecule towards inhibition of corrosion of steel in 0.5 M H2SO4 medium". Progress in organic coatings, 51(2), (2004), 118-124.

[12] Aberchane, M., Fechtal, M., Chaouch, A., Bouayoune, T. "Influence de la durée et de la technique d'extraction sur le rendement et la qualité des huiles essentielles du cèdre de l'Atlas (Cedrus atlantica manetti) ». J Ann. Rech. For. Maroc, 34, (2001), 110-118.

[13] Jaouadi, I., Cherrad, S., Tiskar, M., Tabyaoui, M., Ghanmi, M., Satrani, B., Chaouch, A. "Wood tar essential oil from Cedrus Atlantica of Morocco (Middle atlas) as a green corrosion inhibitor for mild steel in 1 M hydrochloric acid solution". International Journal of Corrosion and Scale Inhibition, 9(1), (2020), 265-283.

[14] N. Nakayama, "Inhibitory effects of nitrilotris(methylenephosphonic acid) on cathodic reactions of steels in saturated Ca(OH)2 solutions", Corrosion Science, 42 (11), (2000), 1897–1920.

[15] Kliškić, M., Radošević, J., Gudić, S., & Katalinić, V. "Aqueous extract of Rosmarinus officinalis L. as inhibitor of Al–Mg alloy corrosion in chloride solution". Journal of applied electrochemistry, 30(7), (2000), 823-830.

[16] O. K. Abiola, N. C. Oforka, E. E. Ebenso, and N. M. Nwinuka, "Eco- friendly corrosion inhibitors: the inhibitive action of Delonix Regia extract for the corrosion of aluminium in acidic media", *Anti-Corrosion Methods and Materials*, 54 (4), (2007), 219–224.

[17] K. A. A. Al-Sodani, O. S. B. Al-Amoudi, M. Maslehuddin, and M. Shameem, "Efficiency of corrosion inhibitors in mitigating corrosion of steel under elevated temperature and chloride concentration", *Construction and Building Materials*, 163, (2018), 97–112.
[18] N. Caliskan and E. Akbas, "The inhibition effect of some pyrimidine derivatives on austenitic stainless steel in acidic media", *Materials Chemistry and Physics*, 126 (3), (2011), 983–988.
[19] R. Cabrera-Sierra, I. García, E. Sosa, T. Oropeza, and I. González, "Electrochemical behavior of carbon steel in alkaline sour environments measured by electrochemical impedance spectroscopy", Electrochimica Acta, 46 (4), (2000), 487–497.
[20] Hernández, H. H., Reynoso, A. M. R., González, J. C. T., Morán, C. O. G., Hernández, J. G. M., Ruiz, Cruz, R. O. "Electrochemical impedance spectroscopy (EIS): A review study of basic aspects of the corrosion mechanism applied to steels". Electrochemical Impedance Spectroscopy, (2020), 137-144.
[21] Hossam, K., Bouhlal, F., Hermouche, L., Merimi, I., Labjar, H., Chaouiki, El Hajjaji, S. "Understanding corrosion inhibition of C38 steel in HCl media by omeprazole: insights for experimental and computational studies". Journal of Failure Analysis and Prevention, 21(1), (2021), 213-227.
[22] De Pauli, M., Gomes, A. M., Cavalcante, R. L., Serpa, R. B., Reis, C. P., Reis, F. T., Sartorelli, M. L. "Capacitance spectra extracted from EIS by a model-free generalized phase element analysis". Electrochimica Acta, 320, (2019), 134366.
[23] L. R. Chauhan and G. Gunasekaran, "Corrosion inhibition of mild steel by plant extract in dilute HCl medium", Corrosion Science, 49 (3), (2007), 1143–1161.
[24] Hmamou, D. B., Salghi, R., Zarrouk, A., Zarrouk, H., Errami, M., Hammouti, Bazzi, L. "Adsorption and corrosion inhibition of mild steel in hydrochloric acid solution by verbena essential oil". Research on Chemical Intermediates, 39(3), (2013), 973-989.
[25] R. Karthikaiselvi and S. Subhashini, "Study of adsorption properties and inhibition of mild steel corrosion in hydrochloric acid media by water soluble composite poly (vinyl alcohol-o-methoxy aniline)", Journal of the Association of Arab Universities for Basic and Applied Sciences, 16, (2014), 74–82.
[26] Bourzi, H., Oukhrib, R., El Ibrahimi, B., Abou Oualid, H., Abdellaoui, Y., Balkard, El Issami, S. "Understanding of anti-corrosive behavior of some tetrazole derivatives in acidic medium: Adsorption on Cu (111) surface using quantum chemical calculations and Monte Carlo simulations". Surface Science, 702, (2020), 121692.
[27] Fariborz Atabaki, S. Jahangiri, and Z. Pahnavar, "Thermodynamic and Electrochemical Investigations of Poly(Methyl Methacrylate–Maleic Anhydride) as Corrosion Inhibitors for Mild Steel in 0.5 M HCl", *Prot Met Phys Chem Surf*, 55 (6), (2019), 1161–1172.
[28] Molhi, A., Hsissou, R., Damej, M., Berisha, A., Thaçi, V., Belafhaili, El Hajjaji, S. "Contribution to the corrosion inhibition of C38 steel in 1 M hydrochloric acid medium by a new epoxy resin PGEPPP". Int. J. Corros. Scale Inhib, 10(1), (2021), 399-418.
[29] N. Labjar, M. Lebrini, C. Jama, F. Bentiss, M. S. Idrissi, and S. El Hajjaji, "Evaluation of the inhibitor synergetic effect of aminotris (methylenephosphonic) acid and metallic salts on the corrosion of iron in acidic medium", Journal of Materials and Environmental Science, (2015).
[30] A. El Bribri, M. Tabyaoui, B. Tabyaoui, H. El Attari, and F. Bentiss, "The use of Euphorbia falcata extract as eco-friendly corrosion inhibitor of carbon steel in hydrochloric acid solution", Materials Chemistry and Physics, 141 (1), (2013), 240–247.

[31] A. Al Maofaria, S. Doucha, M. Benmessaouda, S. E. L. Hajjaji, M. Mosaddak, and B. Ouaki, "Inhibition Study of Various Extracts of Tribulus Terrestris Plant on the Corrosion of Mild Steel in a 1.0 M HCl Solution", *Portugaliae Electrochimica Acta*, 39 (1), (2021), 21–35.
[32] S. Manimegalai and P. Manjula, "Thermodynamic and Adsorption studies for corrosion Inhibition of Mild steel in Aqueous Media by Sargasam swartzii (Brown algae)", (2015), 9.
[33] T. Douadi, H. Hamani, D. Daoud, M. Al-Noaimi, and S. Chafaa, "Effect of temperature and hydrodynamic conditions on corrosion inhibition of an azomethine compounds for mild steel in 1M HCl solution", Journal of the Taiwan Institute of Chemical Engineers, 71, (2017), 388–404.
[34] Babilas, R., Młynarek, K., Łoński, W., Lis, M., Łukowiec, D., Kądziołka-Gaweł, Radoń, A. "Analysis of thermodynamic parameters for designing quasicrystalline Al-Ni-Fe alloys with enhanced corrosion resistance". Journal of Alloys and Compounds, 868, (2021), 159241.
[35] O. Sanni, A. P. I. Popoola, and O. S. I. Fayomi, "Temperature Effect, Activation Energies and Adsorption Studies of Waste Material as Stainless-Steel Corrosion Inhibitor in Sulphuric Acid 0.5 M", J Bio Tribo Corros, 5 (4), (2019).
[36] D. Özkir, E. Bayol, A. A. Gürten, and Y. Sürme, "Thermodynamic study and electrochemical investifation of calcein as corrosion inhibitor for mild steel in hydrochloric acid solution", *Journal of the Chilean Chemical Society*, 58 (4), (2013), 2158–2167.

(2022) ; https://revues.imist.ma/index.php/morjchem